Original Article

www.jmss.mui.ac.ir

Introducing Kernel Based Morphology as an Enhancement Method for Mass Classification on Mammography

Azardokht Amirzadi, Reza Azmi

Department of Computer Engineering, Alzahra University, Iran

Submission: 03-03-2013 Accepted: 14-04-2013

ABSTRACT

Since mammography images are in low-contrast, applying enhancement techniques as a pre-processing step are wisely recommended in the classification of the abnormal lesions into benign or malignant. A new kind of structural enhancement is proposed by morphological operator, which introduces an optimal Gaussian Kernel primitive, the kernel parameters are optimized the use of Genetic Algorithm. We also take the advantages of optical density (OD) images to promote the diagnosis rate. The proposed enhancement method is applied on both the gray level (GL) images and their OD values respectively, as a result morphological patterns get bolder on GL images; then, local binary patterns are extracted from this kind of images. Applying the enhancement method on OD images causes more differences between the values therefore a threshold method is applied toremove some background pixels. Those pixels that are more eligible to be mass are remained, and some statistical texture features are extracted from their equivalent GL images. Support vector machine is used for both approaches and the final decision is made by combining these two classifiers. The classification performance rate is evaluated by A_z, under the receiver operating characteristic curve. The designed method yields $A_z = 0.9231$, which demonstrates good results.

Key words: *Breast cancer, Gaussian Kernel, mammography, mass classification, optical density, structural enhancement*

INTRODUCTION

Breast cancer excludes lung and bronchus cancer has a high mortality rate among woman as American Cancer society reported.[1] The reason is not recognized yet, but early breast cancer detection can be effective in patients' recovery. Despite medical image improvement such as magnetic resonance imaging and ultrasound, mammography is still one of the effective solutions for the detection of breast cancer, and reading mammography images is a demanding job for radiologists. Therefore, computer-aided design (CAD) systems are used to help radiologists in mammography images analysis in the case of breast abnormality detection such as mass, calcification, and architectural distortion.

Since lesion biopsy came to benign in 65-90% of cases, development of the CAD systems is very important in classifying the lesion to malignant and benign in order to reduce unnecessary biopsy. The diagnosis accuracy is increased by merging CAD systems with radiologist knowledge.[2] The CAD effectiveness depends on the accuracy rate of lesion classification and the extracted feature from the mammography images. Mass detection and classification are more challenging tasks than the other abnormalities because masses are not distinguished from the surrounding tissues. Cheng *et al*.[3] presented a review for mass detection and classification methods.

As the contrast of mammography images is mostly low, image enhancement techniques are often used to enhance the images that increase radiologist diagnosis performance and help the CAD systems. An enhancement image is an image in which the observer takes a better perception for the desirable information. In the case of abnormal tissues, structural elements differ from benign masses to malignant ones. Enhancing these structures can cause a better diagnosis rate on mammography images. Since, the Morphological operations are used for different purposes of image processing, mainly image enhancement,[4,5] we introduce a kind of morphological operator in which the primitive structure differs from the past.

The purpose of our method is to enhance suspected lesions so that the early stage diagnosis can be carried out in an effective manner. The new method causes the structural elements to be more visible with the help of morphology operation in which the primitive is estimated by the Gaussian kernel. Local binary pattern (LBP) is extracted from enhanced images, which is a kind of structural texture feature and defines the spatial structure of an

Address for correspondence:
Dr. Azmi, Department of Computer Engineering, Alzahra University, Iran. E-mail:azmi@alzahra.ac.ir

image. LBP has been widely used in face recognition[6-8] and other applications such as cancer detection. In a related work in 2011, Jun Lui *et al*. used an improved LBP in mass classification.[9] The proposed approach also takes advantages from optical density (OD) images,[10] which are free from scanner type and are a measure of blackness[11] that distinguish small differences.[12] In this paper, using this kind of images is shown to be effective and beneficial in mass classification.

The paper is organized as follows. In section 2, necessary pre-processing methods for the classification task are cited. Section 3 describes the proposed approach, and section 4 and 5 include the results and discussion respectively.

MATERIALS AND METHODS

Mammograms Dataset

The mammography cases are from digital database for screening mammography (DDSM), which is publicly available by University of South Florida.[13] The selected cases are taken by different scanners, but they are all digitalized with 12 bit depth and 50 μm pixel size. Some of the images are omitted because of some artifacts such as pencil mark, clips shadow, masses with calcifications, and other abnormalities. The new dataset consists of 516 regions (340 benign and 176 cancers) from 345 patients.

Region of Interest Extraction

The ROI is the same as estimated contour in the DDSM. As the tumor sizes are not in constant ones; therefore, the size of ROI differs from each other. The example of ROI is shown in Figure 1.

Morphological Enhancement

Traditional approaches for image enhancement are good at solving enhancement problems because they are from linear systems. Meanwhile, non-linear geometric approaches are needed in which mathematical morphology techniques are powerful nonlinear methodology.[14]

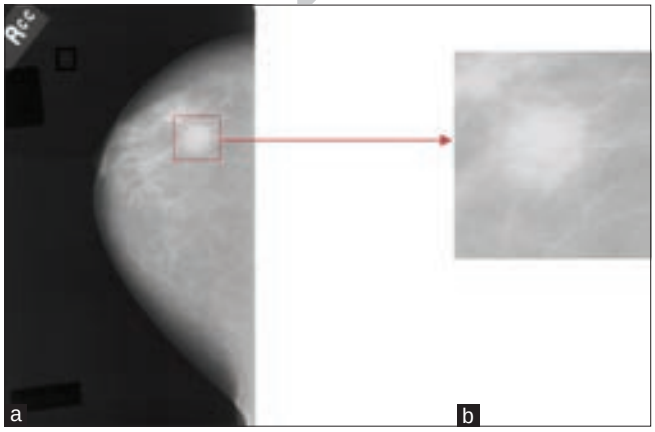

Figure 1: (a) Training image (b) Region of interest from the training image

Some mathematical morphology enhancement techniques are applied in mass classification and segmentation mammography images. As the spicules are the important sign of malignant tumors, enhancing spinal axes of spicules is carried out by the use of morphological skeleton processing.[4] Another study is carried out with a set of morphological operation to remove the lesion background[5] and to enhance the disease patterns.

In this paper, structural morphology enhancement is studied with a new kind of primitive type. More information is presented in the section 3.

Feature Extraction and Selection

Mammography analysis needs the exact description of the ROI, and the texture features are common features in interpreting mammography images. These features are described by a set of statistical, structural, and spectral techniques. In this paper, the statistical and structural ones are used.

The statistical texture features from the ROI are gray level co-occurrence matrix (GLCM),[15,16] gray level run length matrix (GLRLM),[17] and histogram statistics. In this kind of analysis, the features are calculated based on the statistical distribution of the pixel intensity in a given position toward the neighbors in a matrix of the image. The first feature, GLCM, is a table of frequency. In other words, it is the occurrence of pixel intensity value combination estimated in different directions as horizontal, 45, 90 and also 135. It should be noticed that texture is a pattern of pixel intensity in a special direction from a reference pixel. The run length matrix is counted as a number of pixels with the same intensity value in a distinct direction. The third feature describes the intensity distribution over the ROI. The estimated features are as follows: 22 features from the co-occurrence matrix, 11 features from run length matrix, and 6 statistical features. The names of the features are listed in Appendix A.

The structural feature is LBP (Eq. 1, 2). LBP is an operator to describe the spatial structure of an image in which the value of the central pixel (c) from a fixed size window is compared to its neighbors (i_n). Then the value of 0 or 1 is assigned to lower and upper value of the neighbors. These new assignments turn into a decimal number as the LBP feature.[18] Using a 3 × 3 window size produces a 256-bin histogram of the LBP labels.

$$LBP(x_c, y_c) = \sum_{n=0}^{7} 2^n s(i_n - i_c) \quad (1)$$

$$s(u) = \begin{cases} 1, u \geq 0 \\ 0, O.W \end{cases} \quad (2)$$

There are some uniform patterns containing more information than others,[19] which are used here.

Example of the local primitives including different types of curved edges, spots, and flat areas are shown in Figure 2.[20]

Although the input image can be divided in a different window sizes, in this paper, the window is as the size of the ROI.

Proposed Approach

A kind of structural enhancement is proposed to increase breast mass classification performance in which the primitive of morphology operator has been modified. The overview of our method is shown in Figure 3. The new primitive is an optimized Gaussian kernel primitive as the kernel parameters are suited by the genetic algorithm. The proposed primitive is applied on both kinds of images, gray level (GL) and OD. Some texture features are extracted from these images, and finally the support vector machine (SVM) is used as a classifier. In the following scenario, optimizing the primitive elements and extracting features from the GL and OD images are described in details.

Morphology enhancement: Kernel based primitive estimation

Breast tissue has different structural elements. Although some enhancement techniques decrease these structural factors, they increase contrast enhancement. Therefore, a new method is proposed to raise the structural patterns diagnosis. For a better understanding, first morphological filtering theory on gray level (GL) primitive is described and then, the proposed primitive is discussed. As it was mentioned, the structural patterns are discoverable by LBP features; hence, variance of the LBP features is measured to justify the method, which comes at the end of this subsection.

Table 1: Structuring element

0.0498	0.0970	0.0970	0.0498	0.0131	0.0018	0.0001
0.0970	0.2636	0.3679	0.2636	0.0970	0.0183	0.0018
0.0970	0.3679	0.7165	0.7165	0.3679	0.0970	0.0131
0.0498	0.2636	0.7165	1.0000	0.7165	0.2636	0.0498
0.0131	0.0970	0.3679	0.7165	0.7165	0.3679	0.0970
0.0018	0.0183	0.0970	0.2636	0.3679	0.2636	0.0970
0.0001	0.0018	0.0131	0.0498	0.0970	0.0970	0.0498

The GL filters are as follows,[21] if f (x) is the image signal described on continues or discrete plane $E = R^2$ or Z^2 in which $R = \overline{R} \cup \{-\infty, \infty\}$, the most general translation-invariant morphological dilation of a GL image signal f (x) by another signal g is:

$$(f \oplus g)(x) \quad V_{y \in E} f(x-y) + g(y) \tag{3}$$

The structural enhancement is designed by means of dilation operator and Gaussian kernel primitive. The primitive is a 7×7 window in which the elements are computed by 2-D Gaussian kernel.

$$G_{2D}(a, y; \sigma) = -\frac{1}{2\pi\sigma^2} e^{-\frac{x^2+y^2}{2\sigma^2}} \tag{4}$$

In this way, all present elements in the primitive are not treated with the same costs. In other words, the primitive elements are weighting. The further elements take less weight, and those ones, which are spatially near the peak have more values. As dilation operator enlarges the maximum of the function,[21] and also breast masses appear lighter, which are the maximum gray levels in mammography images, applying Gaussian filters act like a hot spot; therefore, breast mass patterns get bolder.

An example of the primitive is shown in Table 1.

Some examples of the enhanced images are displayed in Figure 4.

Variance is used as a measure of diversity, which means more variance causes more diversity on features. In the case of LBP features, more diversity means more patterns are discoverable. To justify the proposed method, one of the common enhancement methods is applied on the images. The common enhancement method adds the original image to the top-hat filtered image and then subtracts the bottom-hat filtered image. Then, the LBP features are extracted from both enhancement methods. Figure 5 shows more variance is achieved by applying the proposed method.

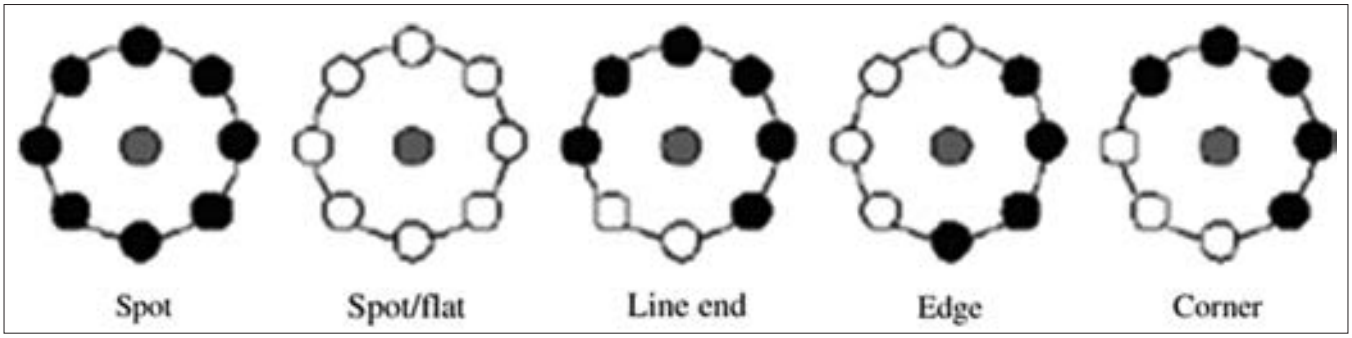

Figure 2: Example of texture primitive

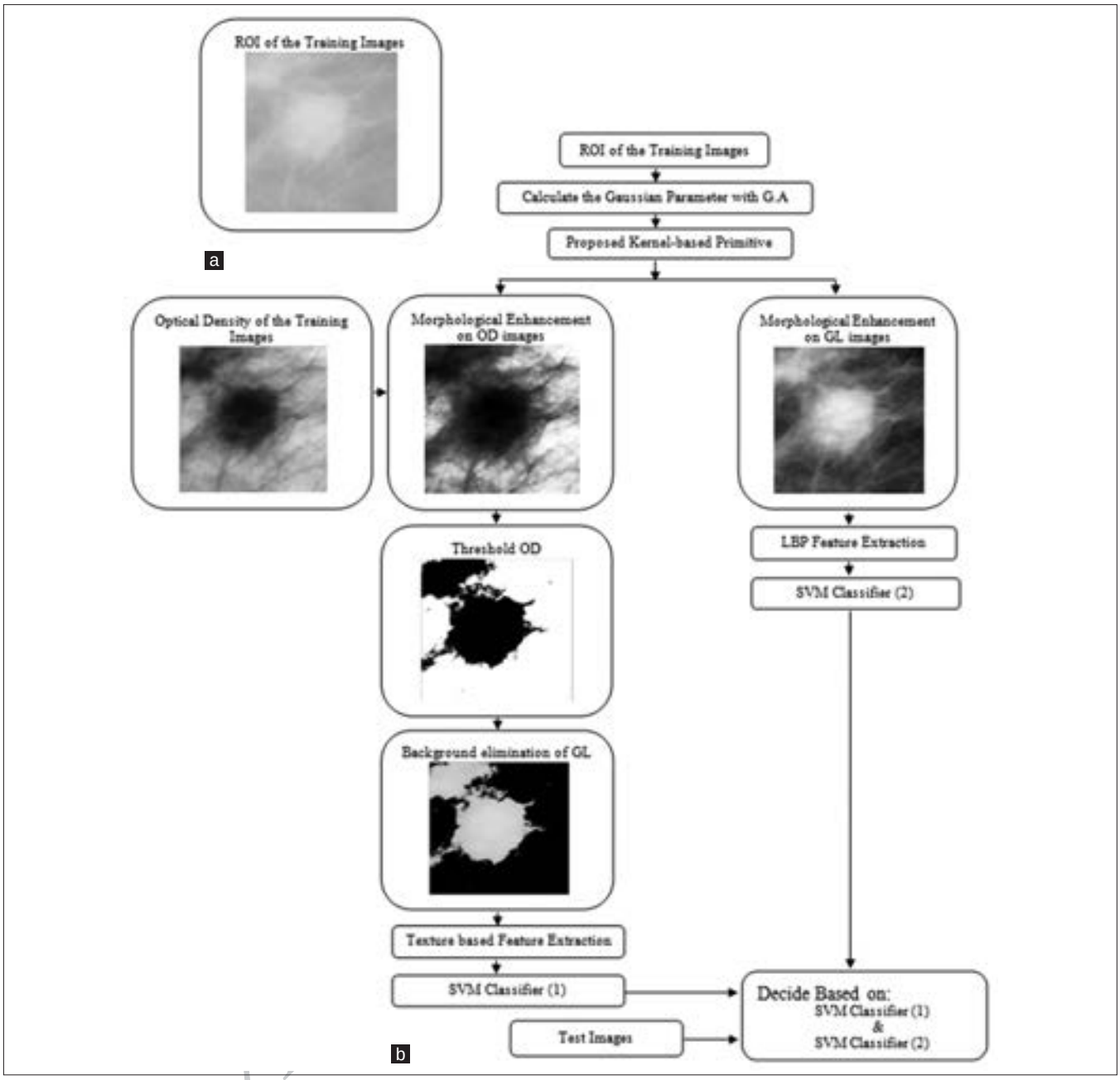

Figure 3: (a) The region of interest of the input image and (b) Illustration of the method

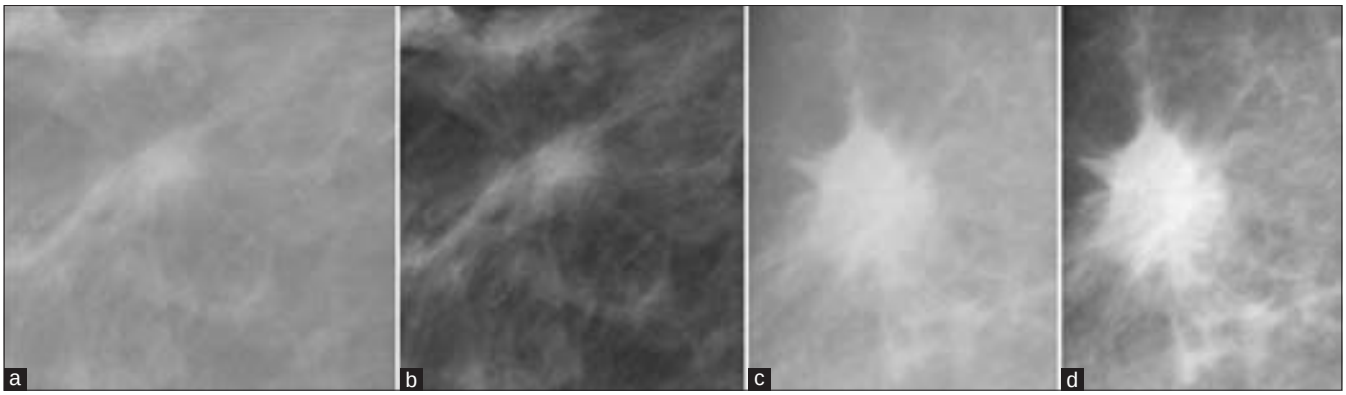

Figure 4: (a) The original image; (b) The enhanced image of A; (c) The original image and (d) The enhanced image

Using OD images to remove GL background

The other proposed technique is to remove mass background with the exploit of OD mammography images. The proposed enhancement method, as mentioned in the previous section, is also applied on OD images-blackness of the processed film. Then a threshold method is assisted to remove the background. The eliminated pixels from the OD images are also removed from the gray level region of interest (GL ROI). As a result, some pixels that are more eligible to be mass are remained on GL ROI. In other words, background is eliminated from GL images. Then some texture based features as statistical, GLCM, and GLRLM are extracted from the GL ROI.

Classification

Among many classifiers, recently SVM is taken much attention in the classification of mammography masses.[9,22,23] The SVM classifier goal is to map features into higher dimensional space while the feature vector is not separable in the original space. SVM classifier is used for both approaches with a linear kernel. For the test image, the two classifiers assign a label. The final decision is made by the maximum probability of the two classes in which the class with more probability assign the final label [Table 2].

RESULTS

In previous sections, the proposed approach was outlined in details. In this section, the classification performance for the two proposed methods on DDSM is evaluated and compared by using 5-fold cross validation and analyzing receiver operating characteristic (ROC) curve. In the following subsections, experimental results are shown as; in section A kernel parameter extraction procedure is described, in section B LBP feature classification on GL images are demonstrated, in section C some texture based features are extracted from OD and GL images, and section D combines the classifiers from two previous subsections and reports the results. However, first of all, the following terms are also used as the evaluation functions:

Table 2: Ensemble classifier algorithm

For all input test images
  SVM classifier (1) assign label1 to input test image
  SVM classifier (2) assign label2 to input test image
  Final label=Label of max (prob-SVM-classifier (1), Prob-SVM-classifier (2))
End

SVM – Support vector machine

$$Accuracy = \frac{TP + TN}{TP + FP + FN + TN} \quad (5)$$

$$FNR = \frac{FN}{FN + TP} \quad (6)$$

$$Sensitivity = TPR = \frac{TP}{TP + FN} \quad (7)$$

$$Specificity = 1 - FPR = \frac{TN}{TN + FP} \quad (8)$$

In this definition, malignant masses are mark as positive values and benign ones as negative. Therefore, false-positive (FP) and false-negative (FN) are two important factors. As FN answers may lead to the patients' death, the FP answers lead to useless biopsy and bring pains for patients. The area under the ROC curve A_z is also used as a factor for the classification performance.

Experimental 1: Kernel Parameter Estimation from GA

In order to select the appropriate Gaussian kernel primitive for the morphological enhancement, genetic algorithm is applied. The value of Mean for the 2-D

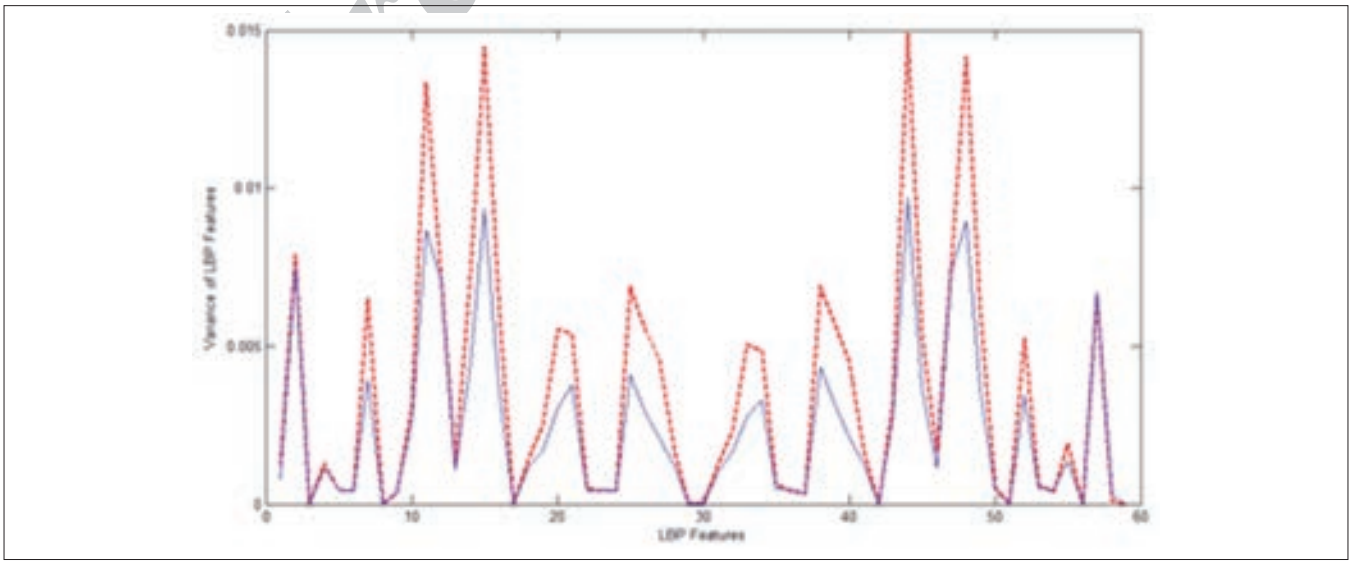

Figure 5: Variance calculated from local binary patterns features, dashed line for the proposed method and the strict line for the common enhancement method

Gaussian kernel is zero in both dimensions as the sigma parameter was learned by Genetic Algorithm. Only 30% of the input dataset is used for the training process. The fitness function is described by the LBP feature variance. The less variance causes more discrimination between the lesions.

Experimental 2: LBP Features on GL Images

The proposed primitive is applied on GL ROIs by dilation operator so the structural patterns are noticeable. Then LBP features are extracted from the GL images. In the case of comparison, the SVM classifies the extracted LBP features from dilated images with different kinds of primitive. The results are shown in Table 3, and its ROC is plotted in Figure 6.

Experimental 3: GLCM, GLRLM and Statistical Texture Based Features on OD and GL Images

As it was mentioned, the second proposed method takes advantages of OD images. In this experiment, the proposed primitive is applied on OD images, and then Otsu's method is applied on the dilated OD images to set the threshold. This causes to remove the background tissue. Now the removed pixels from OD images are also removed from the GL images. This way, the pixels, which are more likely to be mass are remained. Then GLCM, GLRLM and statistical texture based features are extracted from the new images. The SVM classifier is also applied in this step. The table result is shown in Table 4, and its ROC is shown in Figure 7.

Experimental 4: Ensemble the Classifiers

Now, the SVM classifiers from the two previous experiments are joined to get better results. The Final label for the test images is chosen by the maximum probability of the classifiers. Table 5 shows the SVM classifier results in joining the two classifiers from the OD images and their GL ones. Table 5 and Figure 8 show the performance results and the ROC respectively.

Table 3: Result of SVM classifier on LBP features extracted from dilated images

Types of methods	FNR (%)	FPR (%)	Acc (%)	A_z
Original images	29.31	50.21	65.52	0.6481
Disk primitive	27.14	42.01	69.39	0.7271
Diamond primitive	28.99	47.44	66.07	0.6587
Rectangle primitive	26.95	41.75	69.57	0.7307
Proposed primitive	18.09	27.90	78.10	0.8586

SVM – Support vector machine; LBP – Local binary patterns; FNR – False negative rate; FPR – False positive rate; Acc – Accuracy

Table 4: Result of SVM classifier on texture features extracted from the eligible mass region

Types of methods	FNR (%)	FPR (%)	Acc (%)	A_z
Original images	19.00	22.63	79.44	0.8896
Disk primitive	18.70	26.29	78.67	0.8723
Diamond primitive	19.97	30.90	76.55	0.8422
Rectangle primitive	20.81	31.99	75.19	0.8207
Proposed primitive	18.15	21.63	80.63	0.9029

SVM – Support vector machine; FNR – False negative rate; FPR – False positive rate; Acc – Accuracy

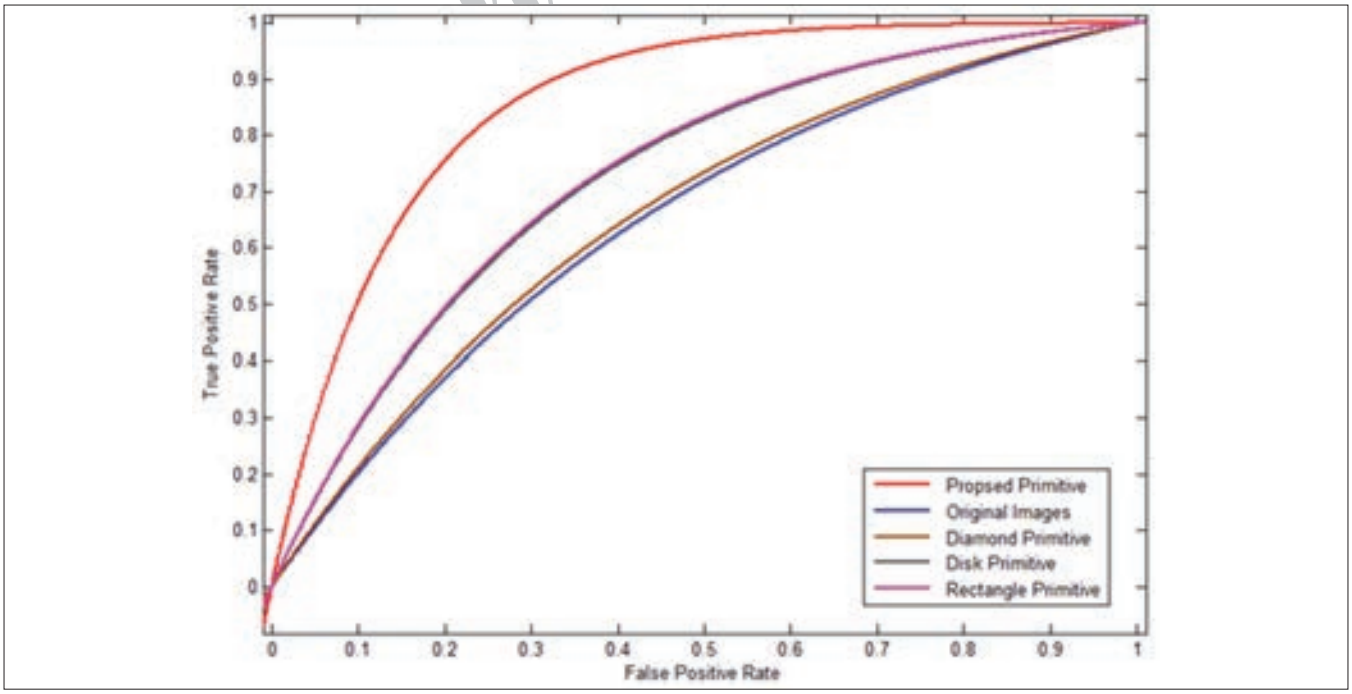

Figure 6: Receiver operating characteristic plot for local binary patterns features

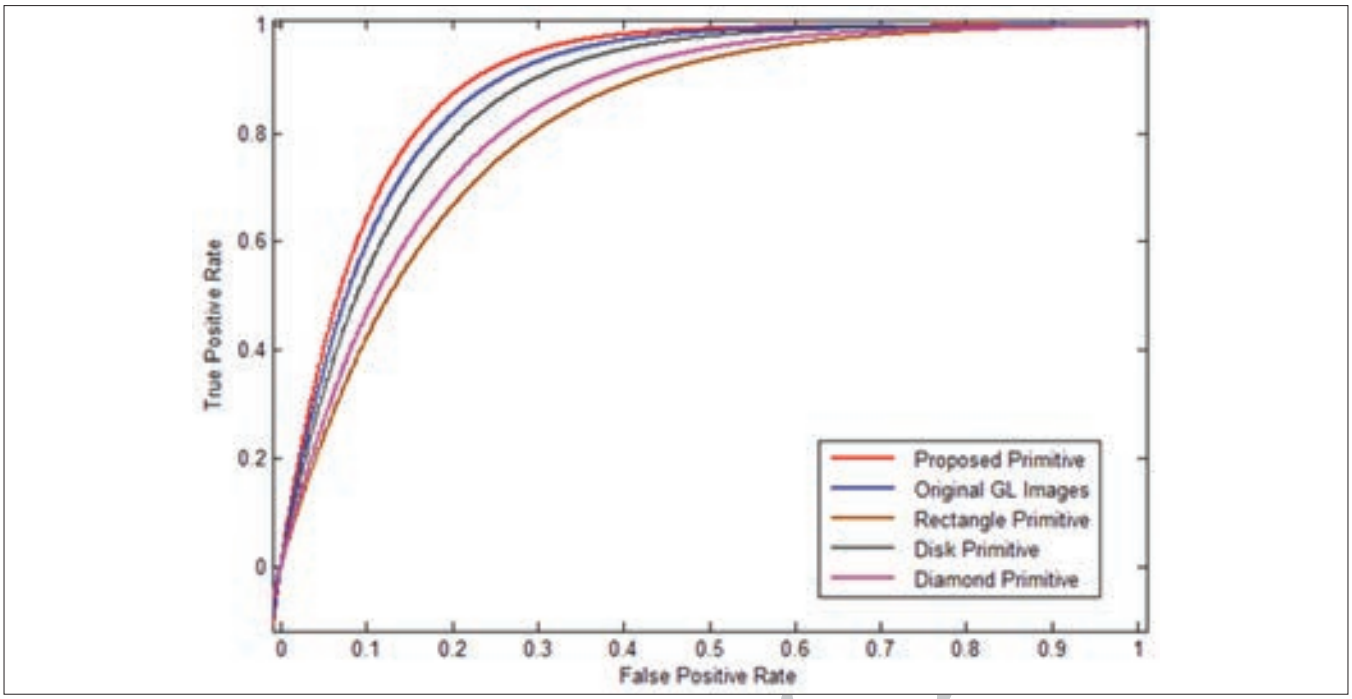

Figure 7: Receiver operating characteristic plot for texture features

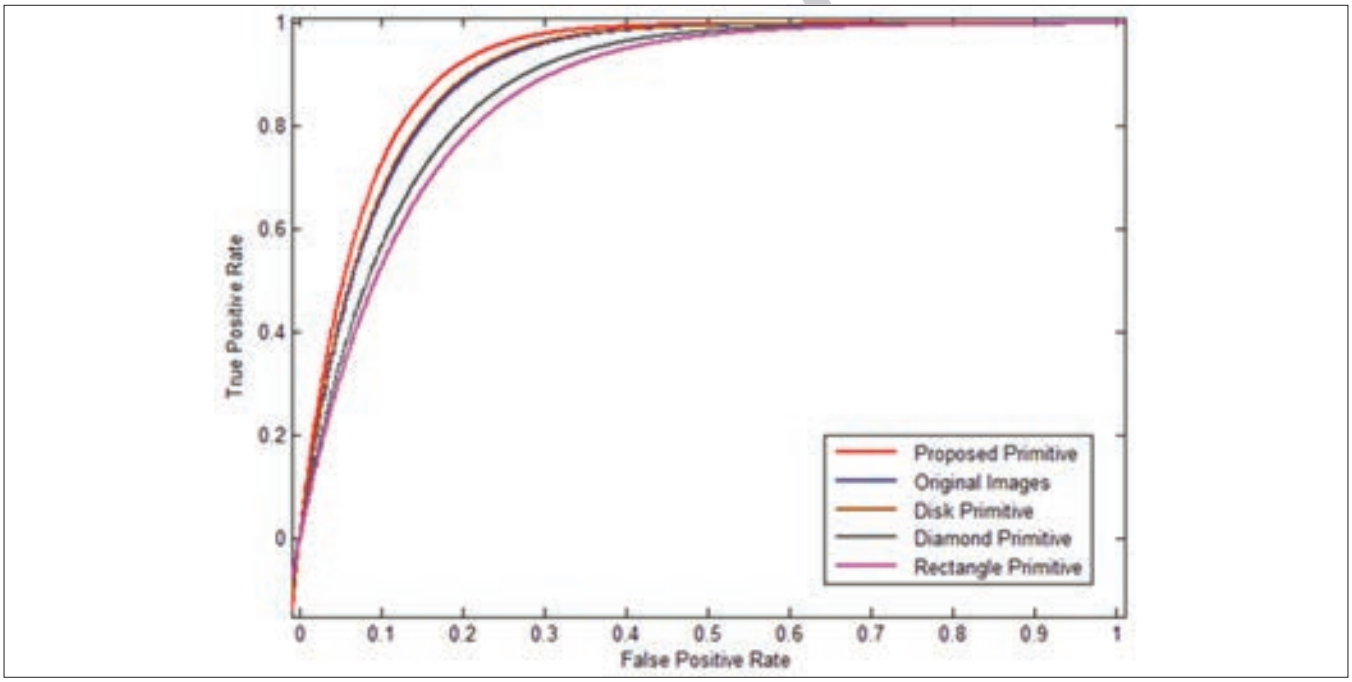

Figure 8: Receiver operating characteristic plot for local binary patterns and texture features

Table 5: Result of SVM classifier on LBP and texture features

Types of methods	FNR (%)	FPR (%)	Acc (%)	A_z
Original images	19.10	20.69	80.42	0.9082
Disk primitive	19.19	20.71	80.43	0.9103
Diamond primitive	20.54	25.03	78.30	0.8809
Rectangle primitive	20.76	26.73	77.50	0.8674
Proposed primitive	17.09	18.25	82.36	0.9231

SVM – Support vector machine; LBP – Local binary patterns; FNR – False negative rate; FPR – False positive rate; Acc – Accuracy

DISCUSSION

All three experiments are evaluated by 5-fold cross validation, and other evaluation measurements, as mentioned, are classification accuracy, False positive rate, False negative rate, and A_z. In the second experiment [Table 2], the LBP features are extracted from the original images and the dilated images with different primitives.

Table 6: Comparison of some recent mass classification methods

Different methods	Feature	Dataset	FNR	FPR	Accuracy	A_z
Our best	LBP, GLCM and GLRLM and statistical texture based features	DDSM	17.09	18.25	82.36	0.9231
Amir Tahmasbi *et al.*[24] (2011)	Zernike moments as shape and density descriptors	MIAS	17.6	18.34	79.83	0.872
Amir Tahmasbi *et al.*[24] (2011)	Zernike moments as shape and density descriptors	MIAS	20.1	16.66	82.14	0.905
Florian Wagner *et al.*[23] (2011)	Intensity transition from the center of a mass up to its surrounding tissue	DDSM	-	-	-	0.77
Rojas *et al.*[25] (2009)	Spiculation measure, fuzziness of mass margins	DDSM, MIAS	-	-	81.0	-
Rangayyan *et al.*[26] (2007)	Fractal dimension, fractional concavity	MIAS	-	-	-	0.82

LBP – Local binary patterns; GLCM – Gray level co-occurrence matrix; GLRLM – Gray level run length matrix; DDSM – Digital database for screening mammography; MIAS – Mammographic image analysis society ; FNR –False negative rate; FPR – False positive rate

The results show that applying dilation operator on original mammography images with two common primitives is better than the pure original image. So dilating mammography images is a good idea. The proposed primitive works well, and classification accuracy rate is increased about 12%. The FNR is decreased about 11%, and also about 23% decrement is reported for the FPR.

In the third experiment [Table 3], the OD images are used to help GL images and remove some background pixels. The results show the proposed primitive works better than the common primitives, which are not good at dilating the OD images. The "original image" means the main GL image without any pixel removing. The present method results show removing some pixels affect about 2% improvement in the classification accuracy rate, and about 1% is decreased in both the FNR and FPR.

In the fourth experiment [Table 4], the two aforementioned features are joined to get a better result. As it is shown, the proposed approach is superior to the common primitives, and A_z achieved to 92.31% in which about 2% increment is perceived. The best values for FNR and FPR is reached to 17.09% and 18.25% respectively. Although they are not noticeable, they are improved about 2% in value.

All in all, dilation operator is used to enhance the morphological patterns of the mammogram images. As it is shown in Table 2, some improvements by the common primitives are gained. Furthermore, the common primitives do not work well for OD images and causes negative effects on the overall classification. The proposed primitives are superior for all the 3 experiments results that show the effective process on OD and GL images.

Comparison of some mass classification methods are shown in Table 6. Many authors only cite the A_z of their proposed method results without any attention to FNR and FPR while they are some important factors in the case of breast mass classification mammography. One of the recent researches by Amir Tahmasbi *et al*.[24] includes these factors. As it is shown in Table 6, the proposed method in this paper has a slight difference in FNR and FPR factors with this recent one, but performs better in A_z.

CONCLUSION

Pre-processing is one of the most essential steps in many applications. In this paper, two new methods are applied; the proposed Gaussian kernel primitive and taking advantages from the OD images. Experimental results demonstrate their good performance on mass classification. The new primitives' elements are trained with genetic algorithm; therefore, they are more powerful than the common primitives. Comparison of the proposed method results is somehow impossible with other works because of different sizes of datasets. As an example, the DDSM has 2620 cases, and only 516 of them are downloaded in this paper. Although we try to increase the classification accuracy rate and decrease FNR and FPR, they did not receive to an acceptable rate. To promote this work, we will add some shape descriptor features in proceeding paper.

REFERENCES

1. Available from: http://www.cancer.org/Research/CancerFactsFigures/CancerFactsFigures/cancer-facts-figures-2012. [Last accessed on 2012 Apr].
2. Doi K. Computer-aided diagnosis: Potential usefulness in diagnostic radiology and telemedicine. Proc Natl Forum 1996;19:9-13.
3. Cheng HD, Shi XJ, Min R, Hu LM, Cai XP, Du HN. Approaches for automated detection and classification of masses in mammograms. Pattern Recognit 2006;39:646-68.
4. Kobatake H, Yoshinaga Y. Detection of spicules on mammogram based on skeleton analysis. IEEE Trans Med Imaging 1996;15:235-45.
5. Li H, Wang Y, Liu KJ, Lo SC, Freedman MT. Computerized radiographic mass detection – Part I: Lesion site selection by morphological enhancement and contextual segmentation. IEEE Trans Med Imaging 2001;20:289-301.
6. Ahonen T, Hadid A, Pietikainen M. Face recognition with local binary patterns. Proc Eur Conf Comput Vis 2004;1:469-81.
7. Ahonen T, Hadid A, Pietikäinen M. Face description with local binary patterns: Application to face recognition. IEEE Trans Pattern Anal Mach Intell 2006;28:2037-41.
8. Nosaka R, Ohkawa Y, Fukui K. Feature extraction based on co-occurrence of adjacent local binary patterns. Pacific-Rim Symp Image Video Technol 2011;7088:82-91.
9. Liu J, Liu X, Chen J, Tang J. Improved local binary patterns for classification of masses using mammography. IEEE Conf 2011;2692-5.

10. Kapur A, Carson PL, Eberhard J, Goodsitt MM, Thomenius K, Lokhandwalla M, *et al*. Combination of digital mammography with semi-automated 3D breast ultrasound. Technol Cancer Res Treat 2004;3:325-34.
11. Parry RA, Glaze SA, Archer BR. The AAPM/RSNA physics tutorial for residents. Typical patient radiation doses in diagnostic radiology. Radiographics 1999;19:1289-302.
12. Haus AG, Yaffe MJ. Screen-film and digital mammography. Image quality and radiation dose considerations. Radiol Clin North Am 2000;38:871-98.
13. Heath M, Bowyer K, Kopans D, Moore R, Kegelmeyer W. The digital database for screening mammography. Proc's 5th Int Workshop Digit Mammography 2001;5:212-18.
14. Maragos PA. Morphological filtering for image enhancement and feature detection. Handbook of Image and Video Processing. 2nd ed. Elsevier Academic; 2005. p. 135-56.
15. Soh L, Tsatsoulis C. Texture analysis of SAR sea ice imagery using gray level co-occurrence matrices. IEEE Trans Geosci Remote Sens 1999;37:780-95.
16. Clausi DA. An analysis of co-occurrence texture statistics as a function of grey level quantization. Can J Remote Sens 2002;28: 45-62.
17. Tang X. Texture information in run-length matrices. IEEE Trans Image Process 1998;7:1602-9.
18. Tan X, Triggs B. Enhanced local texture feature sets for face recognition under difficult lighting conditions. IEEE Trans Image Process 2010;19:1635-50.
19. Ojala T, Pietikainen M, Maenpaa T. Multiresolution gray-scale and rotation invariant texture classification with local binary patterns. IEEE Trans Pattern Anal Mach Intell 2002;24: 971-87.
20. Hadid A, Pietik¨ainen M, Ahonen T. A discriminative feature space for detecting and recognizing faces. IEEE Int Conf Comput Vis Pattern Recognit 2004;2:797-804.
21. Bovik AC. The Essential Guide to Image Processing. Academic Press; 2009.
22. Tang J, Liu X. Classification of breast mass in mammography with an improved level set segmentation by combining morphological features and texture features. Multi Modality State-of-the-Art Medical Image Segmentation and Registration Methodologies. Springer New York 2011. p. 119-35.
23. Wagner F, Wittenberg T. New features for the classification of mammographic masses. Int J Comput Appl 2011;35:29-35.
24. Tahmasbi A, Saki F, Aghapanah H, Shokouhi SB. A novel breast mass diagnosis system based on Zernike moments as shape and density descriptors. IEEE, 18th Iranian Conf. on Biomedical Engineering (ICBME'2011), Tehran, Iran, 2011;18:100-4.
25. Rojas-Domínguez A, Nandi AK. Development of tolerant features for characterization of masses in mammograms. Comput Biol Med 2009;39:678-88.
26. Rangayyan RM, Nguyen TM. Fractal analysis of contours of breast masses in mammograms. J Digit Imaging 2007;20:223-37.

How to cite this article: Amirzadi A, Azmi R. Introducing kernel based morphology as an enhancement method for mass classification on mammography. J Med Sign Sens 2012;3:117-26.
Source of Support: Nil, **Conflict of Interest:** None declared

Appendix A

The texture features used in this paper are as follows:

Statistic
1. Mean
2. Skewness
3. Absolute deviation
4. Variance
5. Kurtosis
6. Standard deviation

Co-occurrence matrix
1. Uniformity/energy/angular second moment
2. Entropy
3. Dissimilarity
4. Contrast/inertia
5. Inverse difference
6. Correlation
7. Homogeneity/inverse difference moment
8. Auto correlation
9. Cluster shade
10. Cluster prominence
11. Maximum probability
12. Sum of squares
13. Sum average
14. Sum variance
15. Sum entropy
16. Difference variance
17. Difference entropy
18. Information measures of correlation (1)
19. Information measures of correlation (2)
20. Maximal correlation coefficient
21. Inverse difference normalized (INN)
22. Inverse difference moment normalized (IDN)

Run-length matrix
1. Short run emphasis (SRE)
2. Long run emphasis (LRE)
3. Gray-level non uniformity (GLN)
4. Run length non uniformity (RLN)
5. Run percentage (RP)
6. Low gray-level run emphasis (LGRE)
7. High gray-level run emphasis (HGRE)
8. Short run low gray-level emphasis (SRLGE)
9. Short run high gray-level emphasis (SRHGE)
10. Long run low gray-level emphasis (LRLGE)
11. Long run high gray-level emphasis (LRHGE)

BIOGRAPHIES

Azardokht Amirzadi received the B.Sc degree in computer engineering from Oloom Fonoon University, Babol, Iran in 2008. Currently she is doing MASc in Artificial Intelligence from Alzahra University, Tehran, Iran. Her research interests include machine learning and computer vision, medical image processing.

E-mail: azardokht_amirzadi@yahoo.com

Reza Azmi received his BS degree in Electrical Engineering from Amirkabir university of technology, Tehran, Iran in 1990 and his MS and PhD degrees in Electrical Engineering from Tarbiat Modares university, Tehran, Iran in 1993 and 1999 respectively. Since 2001, he has joined Alzahra university, Tehran, Iran. He was an expert member of Image Processing and Multi-Media working groups in ITRC (From 2003 to 2004), Optical Character Recognition working group in supreme council of information and communication technology (From 2006 to 2007) and Security Information Technology and Systems working groups in ITRC (From 2006 to 2008). He was Project Manager and technical member of many industrial projects.

E-mail: azmi@alzahra.ac.ir